Journal of Solid State Chemistry **165**, 297–302 (2002)
doi:10.1006/jssc.2002.9533, available online at http://www.idealibrary.com on IDEAL®

Magnetic Behavior of $R_2Ba_2CuPtO_8$ Oxides (R = Ho, Er, Tm, Yb, Lu, and Y)

J. Romero de Paz,* R. Sáez Puche,*,[1] J. L. Martínez,† and E. Baran‡

*Departamento de Química Inorgánica I, Facultad de Ciencias Químicas, Universidad Complutense de Madrid, 28040-Madrid, Spain; †Instituto de Ciencia de Materiales de Madrid, CSIC, 28049 Madrid, Spain; and ‡Química Inorgánica, Facultad de Ciencias Exactas, Universidad Nacional de La Plata, 1900 La Plata, Argentina

Received June 13, 2001; in revised form October 17, 2001; accepted February 8, 2002; published online March 22, 2002

Magnetic properties of polycrystalline $R_2Ba_2CuPtO_8$ (R = Ho, Er, Tm, Yb, Lu and Y) oxides have been studied from magnetization and magnetic susceptibility measurements. The lutetium and yttrium oxides behave as antiferromagnets and the estimated Néel temperatures are 5.2 and 5.7 K, respectively. In the case of the remaining $R_2Ba_2CuPtO_8$ oxides, Cu^{2+} and R^{3+} become antiferromagnetically ordered simultaneously, with the exception of $TmBa_2CuPtO_8$, where the χ vs T plot exhibits two maxima at 8 and 5 K, which have been assigned to the Néel temperatures of Cu^{2+} and Tm^{3+} sublattices, respectively. Taking into account the structure, a superexchange mechanism of the type R–O–Cu–O–R has been proposed in which the Cu^{2+} sublattice plays an important role as promoter of the antiferromagnetic interactions of ferromagnetically R^{3+} coupled in the a–c plane of the structure. Field-induced metamagnetic transitions have been observed below the Néel temperature in all cases; however, different critical fields are achieved depending on the nature of R^{3+} ions. © 2002 Elsevier Science (USA)

Key Words: **copper–lanthanide oxides; superexchange interactions; antiferromagnetism; metamagnetism.**

1. INTRODUCTION

$R_2Ba_2CuPtO_8$ oxides form a family of compounds, where R is one of the smallest rare earths, going from Ho^{3+} to Lu^{3+} and including Y^{3+}. They crystallize with the so-called $Y_2Ba_2CuPtO_8$ structure type, showing orthorhombic symmetry, space group *Pnma* (1, 2). The structure, which is rather complex, can be described as formed by CuO_5 square pyramids and PtO_6 distorted octahedra, which are connected to each other by sharing corners, giving rise to double zigzag chains running parallel to the b-axis, as it is shown in Fig. 1a. The rare-earth atoms, which connect the mentioned double rows, are located in two different crystallographic sites, coordinated to seven oxygen atoms, and form a R_4O_{20} column by edge sharing of the RO_7 monocapped trigonal prism polyhedra.

Very few magnetic studies have been carried out on these complex oxides (3, 4), showing the existence of a rather complex magnetic behavior. This behavior is due to the presence of two kinds of magnetic cations, namely R^{3+} and Cu^{2+}, together with the structural features described above. However, the magnetic characterization of the copper sublattice contribution alone can be analyzed in the case of the $Lu_2Ba_2CuPtO_8$ and $Y_2Ba_2CuPtO_8$ oxides, where rare-earth ions are diamagnetic.

Our preliminary magnetic study of $Lu_2Ba_2CuPtO_8$ and $Er_2Ba_2CuPtO_8$ oxides (4) reveals the existence of antiferromagnetic interactions below 5.2 K in the case of the lutetium compound. In the case of the erbium compound, a field-dependent magnetic behavior is observed below 3 K which corresponds to the Néel temperature (T_N).

The main goal of this paper is to provide new data for a better understanding of the magnetic behavior of this family of compounds. The systematic study of the magnetic properties of $R_2Ba_2CuPtO_8$ (R = Ho, Er, Tm, Yb, Lu and Y) oxides is undertaken from the magnetization and magnetic susceptibility measurements, performed in a wide range of temperatures at different magnetic field strengths.

2. EXPERIMENTAL

The $R_2Ba_2CuPtO_8$ oxides have been obtained as powdered samples from stoichiometric amounts of CuO, R_2O_3, $BaCO_3$ and metallic Pt as fine powder. This mixture was fired in air at 1050°C during 10 days, with intermediate grindings to homogenize and enhance the reaction rate. Further increasing of the mentioned temperature results in the partial decomposition of the $R_2Ba_2CuPtO_8$ phases and increases the amount of impurities in the samples.

The minor amount of impurities detected in the samples can be neglected from the magnetic point of view. In fact, the main impurities identified in the case of the $R_2Ba_2CuPtO_8$

---

[1] To whom the correspondence should be addressed. Fax: (33)-91-394-43-52. E-mail: rsp92@quim.sim.ucm.es.

0022-4596/02 $35.00

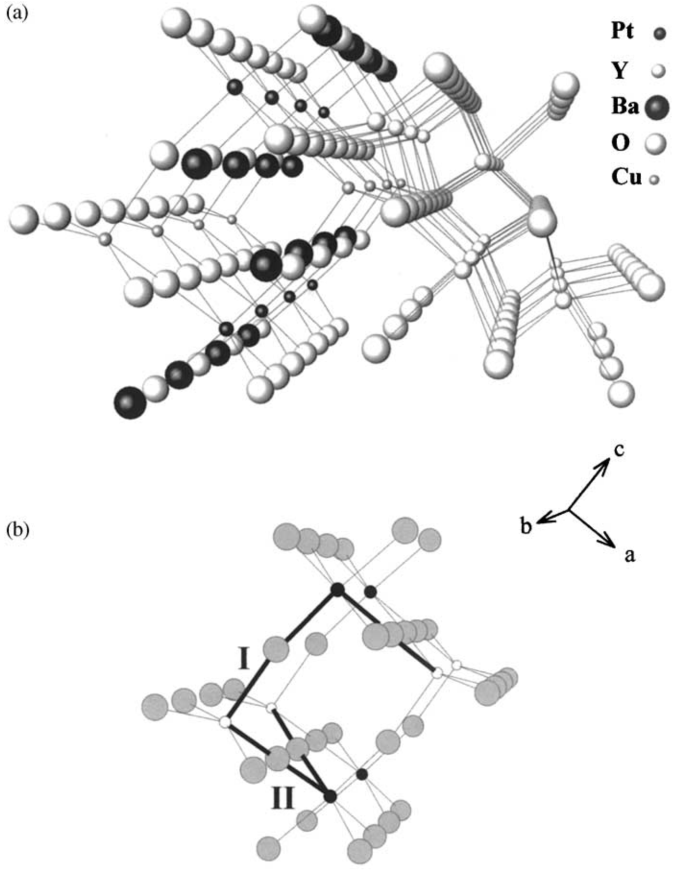

FIG. 1. (a) Crystal structure of $R_2Ba_2CuPtO_8$ (R = Ho, Er, Tm, Yb, Lu, and Y) oxides. (b) The two different pathways of Cu–O–Pt–O–Cu superexchange magnetic interactions.

compounds with R = Yb, Ho and Er have been phases of R_2BaO_4. Small amounts of $Lu_2Ba_4O_7$ and $Tm_4Ba_3O_9$ have been also detected as minor impurities in the $R_2Ba_2CuPtO_8$ (R = Lu and Tm) oxides.

X-ray diffraction data were obtained using a Philips X′ Pert MPD diffractometer and the obtained lattice parameters agree with those published earlier (5). The lattice parameters decrease in the same way as that for the ionic radius of R^{3+} ions going from Gd^{3+} to Lu^{3+}.

DC magnetic susceptibility and magnetization measurements were made in the 2–300 K temperature range using a Quantum Design SQUID MPMS XL magnetometer working at different magnetic fields up to 50 kOe and in a zero-field cooled way. The equipment was calibrated with metallic Pd as standard, and the susceptibility data were corrected taking into account the ionic diamagnetic contributions.

3. RESULTS AND DISCUSSION

Amongst the members of the family of $R_2Ba_2CuPtO_8$ oxides, the Y and Lu oxides represent the simplest cases, since the only paramagnetic cations present in the structure are the Cu^{2+} and both oxides are very suitable to study the magnetism of Cu sublattice without any interference from the rare earths. Figure 2 shows the variation of magnetic susceptibility with temperature for $Y_2Ba_2CuPtO_8$. A net maximum around 6 K can be observed, indicative of the existence of antiferromagnetic order in the copper sublattice below this temperature. The estimated Néel temperatures for the lutetium and yttrium compounds are 5.2 and 5.7 K, respectively. The magnetic susceptibility of both compounds obeys the Curie–Weiss law from 300 to 10 K. The obtained magnetic moments of 2.06 and 1.96 μ_B agree with the expected value for the Cu^{2+} ion, with one unpaired electron located in the $d_{x^2-y^2}$ orbital of the elongated CuO_5 distorted square pyramid. The negative values of Weiss constant of -6.5 and -9.2 K are a consequence of the antiferromagnetic order in both compounds. The magnetization measurements for both compounds have revealed a field-induced transition at about 30 kOe, defined by the presence of a smooth upward deviation from linearity in the M vs H plot, see the inset of Fig. 2.

To explain the antiferromagnetic interactions that take place in the copper sublattice, it is necessary to consider in detail the structure of these compounds, see Fig. 1a. In this sense, Fig. 1b shows that two CuO_5 square pyramids are connected to each other by a PtO_6 octahedron, so the superexchange magnetic interactions take place through the Cu–O–Pt–O–Cu sequence along the b-axis. There are two different pathways (see Fig. 1b): in the first one, the two oxygen atoms involved belong to an axial and an equatorial position of the PtO_6 octahedron, while in the second pathway both oxygen atoms correspond to equatorial positions of the PtO_6 octahedron. In both cases, the Cu–O–Pt–O–Cu angles are very different away from 180° and the relatively large distances are very similar, around 8 Å. All this yields to a poor overlapping between the p orbital of the oxygen atoms and the $d_{x^2-y^2}$ orbital of the copper atoms, justifying the small values found for the T_N in these compounds.

The case of the remaining $R_2Ba_2CuPtO_8$ oxides is rather complex, since two paramagnetic cations, R^{3+} and Cu^{2+}, are involved. The magnetic behavior of the described $R_2Ba_2CuPtO_8$ (R = Lu and Y) phases is strongly modified after the substitution of the nonmagnetic Lu^{3+} and Y^{3+} cations by other paramagnetic R^{3+} cation. As we will discuss later, the different nature of the paramagnetic R^{3+} cation strongly influences the magnetic behavior of these oxides at lower temperatures.

In fact, the $R_2Ba_2CuPtO_8$ (R = Ho, Er, Tm and Yb) follow the Curie–Weiss behavior, $\chi = C/(T + \Theta)$, over 100–300 K temperature range, and the values of C and Θ obtained for each oxide are shown in Table 1. The obtained magnetic moment for R^{3+}, after discounting the Cu^{2+} contribution, agrees with that calculated for the R^{3+} ion using the Hund equation, see Table 1. On the other

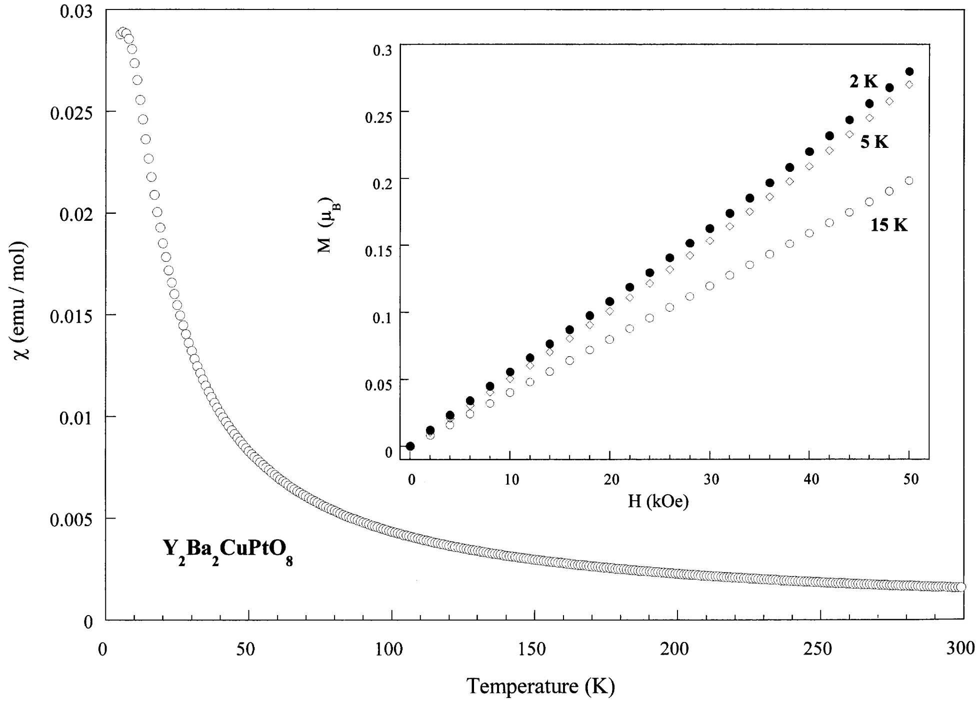

FIG. 2. Temperature dependence of the magnetic susceptibility for $Y_2Ba_2CuPtO_8$ oxide. The inset shows the magnetization isotherms at 2, 5 and 15 K.

hand, in all cases, the magnetic susceptibility shows a net maximum that is indicative of the existence of antiferromagnetic order in which both rare-earth and copper sublattices are involved. The estimated Néel temperatures and Weiss constants are included in Table 1. This behavior qualitatively remains to the one, previously discussed for the isostructural lutetium and yttrium compounds. However, with the exception of the ytterbium compound, the magnetic susceptibility shows rather interesting field dependence.

The magnetic susceptibility of $Yb_2Ba_2CuPtO_8$ oxide shows a net maximum at 4 K, Fig. 3, and the deviations downwards of the linearity below 60 K are due to the crystal field (CF) effect on ${}^2F_{7/2}$ ground term of Yb^{3+}. It is noted that the effect of the CF on the ground term of Yb^{3+} is the largest compared with the other trivalent lanthanide cations. In fact from the Mössbauer spectroscopy, measurements have been determined that the first exited crystal-field doublet is separated from the ground-state doublet by an amount of 100 K (9) in the case of Yb_2BaNiO_5, where the Yb is sevenfold coordinated by oxygen as in this case. This relatively large crystal-field splitting means that in the temperature range where the magnetic ordering takes place, only the ground Kramers doublet is populated and this justify the low Néel temperatures reported for the yterbium oxides. The maximum found at 4 K has been assigned to the T_N and below this temperature both Yb^{3+} and Cu^{2+} sublattices are antiferromagnetically correlated. In this sense, we have previously reported for some mixed oxides of general formula Yb_2BaMO_5 (M: Co, Ni, Cu) (6–8), the role of the M^{2+} ions as a promoter of the interactions in the Yb^{3+} sublattice. It is worth noting that the estimated T_N of $Yb_2Ba_2CuPtO_8$ oxide is higher than that one reported for Yb_2BaMO_5 oxides. Moreover, in the case of the two polymorphic phases of Yb_2BaNiO_5 no order has been found down to 50 mK (personal communication) for the so-called *Pnma* phase, while in the case of the *Immm* phase three-dimensional antiferromagnetic ordering has been recently reported below 8.7 K (9). The magnetization vs field measurement at different temperatures, inset of Fig. 3, reveals the presence of metamagnetism below 50 kOe. The M vs H plot obtained at 2 K has a characteristic S shape

TABLE 1

Curie and Weiss Constants, Experimental and Theoretical Magnetic Moments of R^{3+} Ions per Formula Unit, Néel Temperature and Experimental- and Theoretical-Ordered Magnetic Moments of $R_2Ba_2CuPtO_8$ (R = Y, Ho, Er, Tm, Yb, and Lu) Oxides

Compound	C (emu K mol^{-1})	θ (K)	$\mu_{exp.}$ (μ_B)	$\mu_{theor.}$ (μ_B)	T_N (K)	$\sigma_{exp.}$ (μ_B)	$\sigma_{theor.}$ (μ_B)
$Y_2Ba_2CuPtO_8$	0.48	− 9.2	1.96	1.73	5.7	—	1
$Ho_2Ba_2CuPtO_8$	26.6	− 1.5	14.4	14.9	10	—	14.2
$Er_2Ba_2CuPtO_8$	22.3	− 8.8	13.2	13.5	3	9.7	12.8
$Tm_2Ba_2CuPtO_8$	11.5	− 5.2	9.4	10.6	8.2; 4.5	6.4	9.9
$Yb_2Ba_2CuPtO_8$	6.2	− 84	6.7	6.4	4	2.0	5.7
$Lu_2Ba_2CuPtO_8$	0.53	− 6.5	2.06	1.73	5.2	—	1

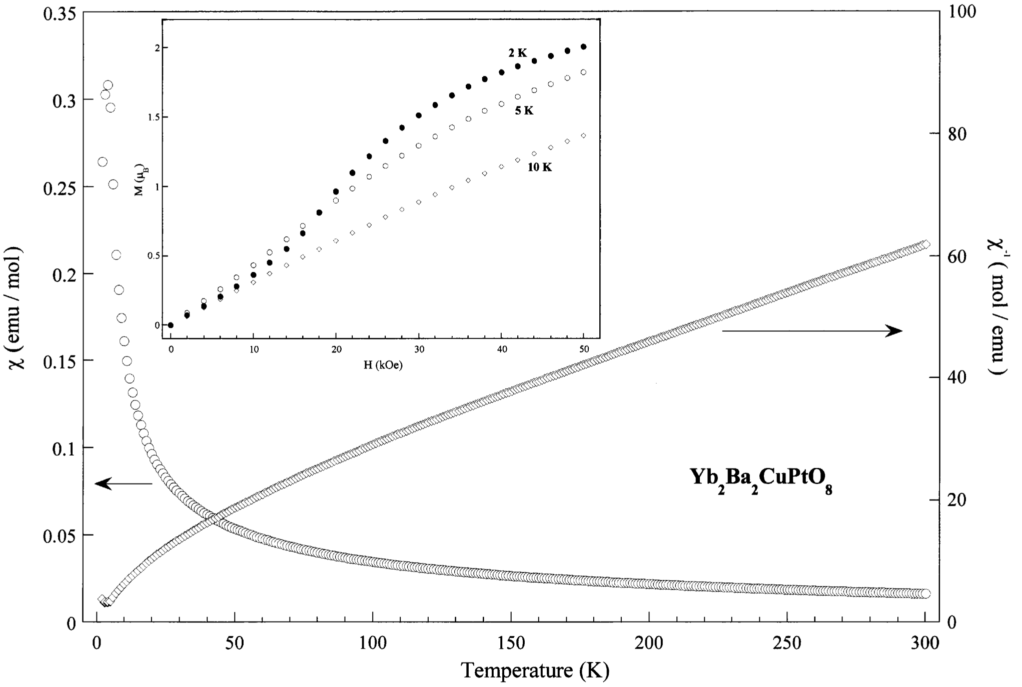

FIG. 3. Temperature dependence of the magnetic susceptibility and its inverse for $Yb_2Ba_2CuPtO_8$ oxide. The inset shows the magnetization vs magnetic field measurements at 2, 5 and 10 K.

and the estimated critical field is 15 kOe. The extrapolation of the magnetic moment in the 30–50 kOe field range yields an ordered moment of about 2 μ_B, see Table 1.

The magnetic behavior of $Tm_2Ba_2CuPtO_8$ oxide is rather complex. The magnetic susceptibility below 60 K is dependent on the magnetic field strength, as it can be observed in

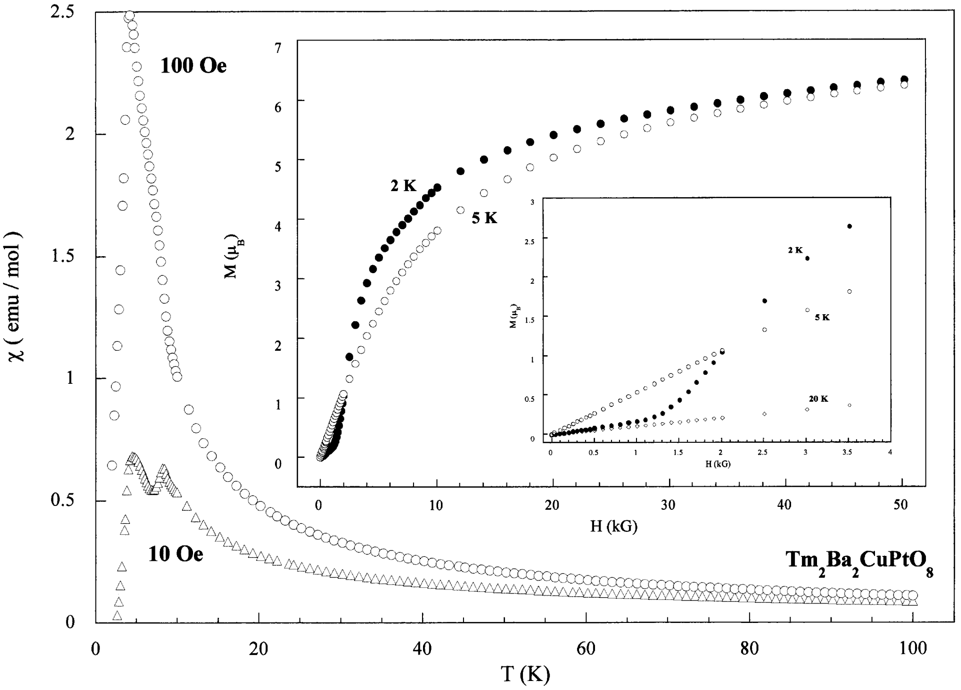

FIG. 4. Temperature variation of magnetic susceptibility of $Tm_2Ba_2CuPtO_8$ oxide measured at 10 and 100 Oe. The inset shows the magnetization vs magnetic field measurements at 2 and 5 K and the low-magnetic field dependence at 2, 5 and 20 K.

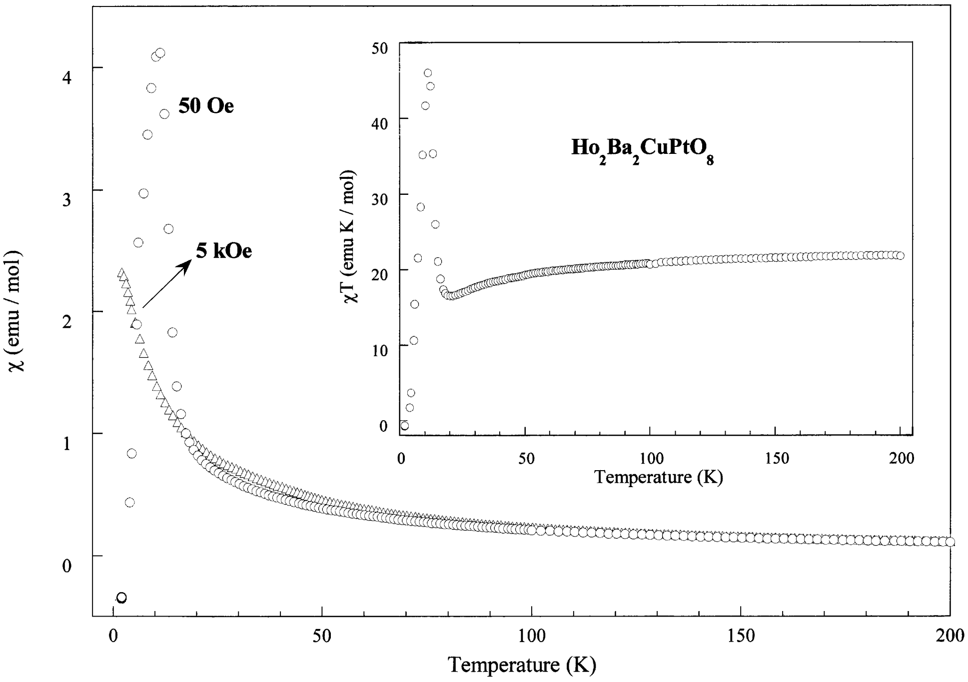

FIG. 5. Temperature variation of magnetic susceptibility of $Ho_2Ba_2CuPtO_8$ oxide measured at 50 Oe and 5 kOe. The inset shows the χT variation vs temperature at 50 Oe.

Fig. 4. When the external magnetic field is 10 Oe, two well-defined and separated maxima are observed at 8.2 and 4.5 K. By increasing the field, the maximum observed at 8.2 K is partly masked due to the appearance of a weak field-induced ferromagnetic component, and just a hump is clearly visualized, but the net maximum at about 4 K remains. These results suggest the operations of antiferromagnetic correlations in the copper sublattice at 8.2 K, which is forming an infinite zigzag chain along the *b*-axis, as we have already discussed in the case of the isostructural yttrium and lutetium compounds. When temperature decreases, the copper promotes the correlations in the Tm^{3+} sublattice and at 4 K both Tm^{3+} and Cu^{2+} sublattices are antiferromagnetically correlated. Very recently, neutron diffraction data taken in the isostructural $Ho_2Ba_2CuPtO_8$ oxide (unpublished results) support our assumption. On the contrary, a decade ago, Toyota *et al.* (3) found similar magnetic behavior, but they proposed a different antiferromagnetic model in which the coupling between Er^{3+} and Cu^{2+} was independent in the case of the analogous $Er_2Ba_2CuPtO_8$.

On the other hand, the ferromagnetic component induced by the magnetic field as low as 100 Oe can be clearly visualized as a jump in the χT vs T plot. This induced ferromagnetic behavior is confirmed from the M vs H measurements at different temperatures, inset of Fig. 4. The magnetization isotherms obtained below the T_N, namely at 2 and 5 K, are similar and above 40 kOe are almost coincident and tend to saturate up to 50 kOe. The obtained moment value of 6.4 μ_B at 50 kOe is smaller than that expected for two Tm^{3+}, see Table 1. In fact, the contribution to the magnetic moment from Tm^{3+} appears to be a function of the crystallographic site and the obtained results can be explained taking into account only one Tm^{3+} ion. Similar results have been recently obtained from neutron diffraction studies in the case of the Yb_2BaCoO_5 oxide (6), where the saturation magnetic moment was explained considering only the magnetic contribution of Yb(2), while the Yb(1) contribution was almost zero. A crossover around 2000 Oe can be observed in the inset of Fig. 4 and the data obtained at 2 K became higher than those obtained at 5 K for H values higher than 2000 Oe. These data are rather unusual for a ferromagnetic compound. The lineal variation at 2 K between 0 and 1000 Oe is characteristic of an antiferromagnetic material, but at 1200 Oe a break is observed and the magnetization suddenly increases. This behavior suggests that the spin-flipping to a meta-magnetic phase has been induced around 1200 Oe.

$Er_2Ba_2CuPtO_8$ and $Ho_2Ba_2CuPtO_8$ oxides show a similar magnetic behavior. In a previous work, a detailed study of the former has been done (3, 4) and the magnetization on a single crystal of $Er_2Ba_2CuPtO_8$ reveals important anisotropic effects. A model of antiferromagnetic ordering of ferromagnetically coupled Er^{3+} moments with its easy axis in the *a*–*c* plane is proposed (3).

For $Ho_2Ba_2CuPtO_8$ oxide, the magnetic susceptibility is field dependent, as can be observed in Fig. 5. The χ vs T plot obtained at 50 Oe shows the appearance of a ferromagnetic component at 15 K followed by a net maximum at 10 K, which is due to the presence of antiferromagnetic interactions in the Cu^{2+} and Ho^{3+} sublattices. The presence of this ferromagnetic component is better visualized in the $\chi\ T$ vs T plot, inset of Fig. 5. However, the susceptibility data obtained at 5000 Oe do not show evidence of the ferromagnetic correlations detected using lower magnetic fields. As it was proposed in the case of the $\mathrm{Er_2Ba_2CuPtO_8}$ oxide, this magnetic field seems to be enough to suppress the ferromagnetic component that is present in these compounds and the antiferromagnetic interactions that take place at lower temperatures.

4. CONCLUSIONS

We have studied the magnetic behavior of the family of compounds $R_2\mathrm{Ba_2CuPtO_8}$ (R: rare earth). Both magnetization and magnetic susceptibility measurements over a wide range of temperature and at different magnetic fields, indicate that in the case of $R_2\mathrm{Ba_2CuPtO_8}$ ($R =$ Y and Lu) the Cu^{2+} becomes antiferromagnetically ordered at 5.7 and 5.2 K, respectively. This low T_N has been explained taking into account the isolated $\mathrm{CuO_5}$ square pyramids and the complex exchange pathway through which the interactions take place. The substitution of these two mentioned diamagnetic rare earths by a paramagnetic R^{3+} ion, the remaining $R_2\mathrm{Ba_2CuPtO_8}$ ($R =$ Ho, Er, Tm and Yb) oxides, yields important changes in the magnetic behavior. The Cu^{2+} sublattice induces moment on the R^{3+} sublattice and the obtained data appear to confirm the model of totally antiferromagnetic ordering of ferromagnetically coupled R^{3+} in the a–c plane of the structure.

ACKNOWLEDGMENTS

The authors are indebted to CICYT for financial support under Project No. MAT2000-0753-C02-01.

REFERENCES

1. J. S. Swinnea and H. Steinfink, *Acta Crystallogr. C* **43,** 2436 (1987).
2. K. Kato, K. Kosuda, Y. Uchida, E. Takayama-Muromachi, and O. Fukunaga, *Acta Crystallogr. C* **44,** 794 (1988).
3. N. Toyota, C. van den Beek, J. A. Mydosh, P. Koorevaar, J. van den Berg, P. Kes, Y. Nishihara, K. Murata, T. Shisido, Y. Saito, K. Ukei, T. Sasaki, H. Iwasaki, and T. Fukuda, *J. Magn. Magn. Mater.* **90&91,** 237 (1990).
4. E. J. Baran, J. Romero, R. Sáez Puche, and J. L. Martínez, *J. Alloys Compds.* **275–277,** 127 (1998).
5. M. B. Vasallo and E. J. Baran, *J. Solid State Chem.* **120,** 316 (1995).
6. J. Hernández-Velasco, R. Sáez-Puche, and J. Rodríguez-Carvajal, *J. Alloys Compds.* **275–277,** 651 (1998).
7. R. Sáez-Puche, J. M. Coronado, C. L. Otero-Díaz, and J. M. Martín-Llorente, *Mater. Chem. Phys.* **34,** 233 (1993).
8. A. Salinas-Sánchez, R. Sáez-Puche, and M. A. Alario-Franco, *J. Solid State Chem.* **89,** 361 (1990).
9. J. A. Hodges, P. Bonville, N. Genand-Riondet, K. Tomala, N. Kernavanois, E. Ressouche, J. P. Sánchez, and P. Vulliet, *J. Phys.: Condens. Matter* **12,** 9973 (2000).